

Contents lists available at [ScienceDirect](#)

Journal of Sound and Vibration

journal homepage: www.elsevier.com/locate/jsvi

Rapid Communication

Free linear vibrations of cables under thermal stress

Fabien Treysède

Nantes Atlantique University, Laboratoire Central des Ponts et Chaussées, BP 4129, 44341 Bouguenais, France

ARTICLE INFO

Article history:

Received 5 December 2008

Received in revised form

8 June 2009

Accepted 6 July 2009

Handling Editor: M.P. Cartmell

Available online 31 July 2009

ABSTRACT

This paper aims at investigating the effect of thermal stress on free linear vibrations of cables. An analytical model extending Irvine's theory to thermoelasticity is proposed. In addition to the sag-extensibility parameter, this model yields a second dimensionless independent parameter related to the temperature change. Some general two-dimensional contour plots are presented giving the relative change in natural frequencies due to temperature with respect to the only two independent parameters of the problem. Depending on their values, this change can be quite significant. For in-plane symmetric modes, it is shown that a positive (resp. negative) temperature change does not necessarily decrease (resp. increase) natural frequencies and that thermoelastic effects can lead to cross-over due to the modification of the initial sag.

© 2009 Elsevier Ltd. All rights reserved.

1. Introduction

Cables are widely used in modern structures (bridges, post-tensioned concrete, suspended roofs, skylifts, elevators). The study of their vibrations has a long history, since the eighteenth century (see Refs. [1,2]). Irvine's work [1] is probably one of the most important contributions, its main advantage being that only one dimensionless parameter (namely, the sag-extensibility parameter) is needed to determine cable natural frequencies. Since then, many studies have aimed at taking into account more complicated mechanics by including bending stiffness [3,4] or nonlinear dynamics effects [5–9] for instance. However, to the author's knowledge, the investigation of thermal effects on cable dynamics has surprisingly not received a similar attention in the literature. The goal of this paper is to extend Irvine's model to thermally stressed cables.

One of the motivations is the potential need of adequate models for vibration based methods in structural health monitoring (SHM). These methods are potentially attractive for tension estimation [10,11] or damage detection [12,13] in cables, but are likely to suffer a lack of robustness because of environmental temperature change (affecting the initial cable tension and in turn its modal parameters). It is well-known that differentiating changes due to the environment from changes due to damage is still a challenging task [14–17]. In addition to SHM, one could also note that temperature changes may also affect the robustness of vibration control strategies [18,19].

This study focuses on moderate thermal stress typically due to climatic variations. In Section 2, the thermoelastic equilibrium equations are derived both for cable statics and linear dynamics. A second independent parameter, related to temperature change, is naturally introduced. Section 3 gives general contour plots of the relative change in natural frequencies with respect to the only two independent parameters of the problem. Section 4 finally concludes this paper.

E-mail address: fabien.treysede@lpc.fr

2. Theory

Fig. 1 depicts the cable profile for its three equilibrium states: the initial static state (without thermal change), the thermally stressed static state and the superimposed dynamic state. The present study is restricted to small linear superimposed vibrations.

2.1. Statics without thermal stress

We consider a suspended cable anchored on supports at the same level, l being its span. Due to its own weight, the cable has a sag, denoted d . H is the horizontal component of the external applied tension. τ is the tension inside the cable (the notation T is usually chosen in the literature but, in this paper, it will be kept for temperature). mg is the self-weight of the cable per unit length. The static equilibrium of the cable is given by [1]

$$\frac{d}{ds} \left(\tau \frac{dx}{ds} \right) = 0, \quad \frac{d}{ds} \left(\tau \frac{dz}{ds} \right) = -mg \quad (1)$$

yielding

$$\tau \frac{dx}{ds} = \text{cst} = H, \quad H \frac{d^2 z}{dx^2} = -mg \sqrt{1 + \left(\frac{dz}{dx} \right)^2} \quad (2)$$

where we have used the equality $ds/dx = \sqrt{1 + (dz/dx)^2}$, obtained from the geometric constraint $(dx/ds)^2 + (dz/ds)^2 = 1$. For small sag (typically, $d/l < 1/8$), one can assume $(dz/dx)^2 \ll 1$ and the static equilibrium equation simplifies into [1]

$$H \frac{d^2 z}{dx^2} = -mg \quad (3)$$

The boundary conditions are

$$z(0) = z(l) = 0 \quad (4)$$

The solution for the cable profile is then

$$z(x) = \frac{mgl^2 x}{2H l} \left(1 - \frac{x}{l} \right) \quad (5)$$

and the sag is

$$d = z(l/2) = mgl^2 / 8H \quad (6)$$

One must have $H > mgl$ (in order for d/l to be less than $1/8$). The cable length is $L = \int_0^l \sqrt{1 + (dz/dx)^2} dx$, which can be approximated by a first-order Taylor expansion as

$$L = l \left(1 + \frac{m^2 g^2 l^2}{24H^2} \right) \quad (7)$$

2.2. Thermally stressed state

Under thermal stress, an increment h (positive or negative depending on the sign of temperature change) is added to the initial applied tension H . The static equilibrium now reads

$$\frac{d}{ds} \left((\tau + \tau') \left(\frac{dx}{ds} + \frac{du}{ds} \right) \right) = 0, \quad \frac{d}{ds} \left((\tau + \tau') \left(\frac{dz}{ds} + \frac{dw}{ds} \right) \right) = -mg \quad (8)$$

where u and w are the additional longitudinal and vertical cable displacement owing to temperature effects. τ' is the additional tension in the cable. Neglecting u and taking into account Eq. (2), the first equation in (8) becomes

$$\tau' \frac{dx}{ds} = h \quad (9)$$

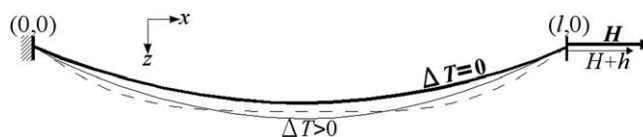


Fig. 1. Cable profile for the initial static equilibrium state (thick line), thermally stressed state (thin line) and dynamic state (dashed line). The figure gives an example for a positive thermal change, corresponding to a decrease in the applied tension at the end and an increase of sag. The dynamic profile here corresponds to a second symmetric in-plane mode.

and using the same simplifications as before, Eqs. (8) yield the following equilibrium equation:

$$(H + h) \frac{d^2}{dx^2} (z + w) = -mg \tag{10}$$

with boundary conditions

$$w(0) = w(l) = 0 \tag{11}$$

Taking into account the equilibrium state (3) into (10), integrating and using boundary conditions (11) yields

$$w(x) = -\frac{h}{H + h} z(x) \tag{12}$$

At this stage, h is still unknown and must be evaluated. Denoting ΔT as the temperature change (assumed uniform throughout this paper), the generalized Hooke's law of linear thermoelasticity stipulates that [20]

$$\tau + \tau' = EA(\varepsilon + \varepsilon' - \alpha\Delta T) \tag{13}$$

where $\tau = EA\varepsilon$ from the initial equilibrium state (ε being the initial strain). E , A and α respectively denote the Young modulus, the cross-section area and the thermal expansion coefficient. ε' is the additional thermal strain:

$$\varepsilon' = \frac{ds'^2 - ds^2}{2ds^2} \tag{14}$$

where ds is the original length of the element before temperature change and ds' is its new length:

$$ds^2 = dx^2 + dz^2, \quad ds'^2 = (dx + du)^2 + (dz + dw)^2 \tag{15}$$

Using Eqs. (14), (15), (9), and ignoring the high-order term $(du/dx)^2/2$, Eq. (13) yields after multiplication by $(ds/dx)^2$:

$$\frac{h}{EA} \left(\frac{ds}{dx}\right)^3 = \frac{du}{dx} + \frac{dz}{dx} \frac{dw}{dx} + \frac{1}{2} \left(\frac{dw}{dx}\right)^2 - \alpha\Delta T \left(\frac{ds}{dx}\right)^2 \tag{16}$$

Integrating from 0 to l and by parts the second term of the right hand side gives

$$\frac{hL_e}{EA} = u(l) - u(0) + \frac{mg}{H} \int_0^l w dx + \frac{1}{2} \int_0^l \left(\frac{dw}{dx}\right)^2 dx - \alpha\Delta T L_t \tag{17}$$

where $L_e = \int_0^l (ds/dx)^3 dx$ and $L_t = \int_0^l (ds/dx)^2 dx$. From $ds/dx = \sqrt{1 + (dz/dx)^2}$, we have (Taylor expansion)

$$L_e = l \left(1 + \frac{m^2 g^2 l^2}{8H^2}\right), \quad L_t = l \left(1 + \frac{m^2 g^2 l^2}{12H^2}\right) \tag{18}$$

It might be useful to consider flexible horizontal supports at the ends, simply modelled as linear springs of stiffness k_0 and k_l :

$$h = k_0 u(0), \quad \bar{h} = -k_l u(l) \tag{19}$$

Using Eqs. (5), (12) and (19) into (17) finally gives the following equation for the additional tension:

$$h^{*3} + (2 + \theta + \lambda^2/24)h^{*2} + (1 + 2\theta + \lambda^2/12)h^* + \theta = 0 \tag{20}$$

where $h^* = h/H$, $\lambda^2 = (mgl/H)^2 l / (HL_e/E_{eq}A_{eq})$, $\theta = \alpha\Delta T L_t / (HL_e/E_{eq}A_{eq})$, and $E_{eq}A_{eq} = EA / \{1 + (1/k_0 + 1/k_l)EA/L_e\}$. λ^2 is the Irvine sag-extensibility parameter. θ is a dimensionless parameter related to the temperature change. Note that $\theta = 0$ yields $h^* = 0$. It is emphasized that Eqs. (12) and (20) are equivalent to the result given without proof in Exercise 2.5 of Irvine's book [1] (the present form being more compact).

2.3. Free linear vibrations under thermal stress

The dynamic equilibrium of the cable is given by the following equations:

$$\frac{d}{ds} \left\{ (\tau + \tau' + \tilde{\tau}) \left(\frac{dx}{ds} + \frac{du}{ds} + \frac{d\tilde{u}}{ds} \right) \right\} = m \frac{\partial^2 \tilde{u}}{\partial t^2} \tag{21}$$

$$\frac{d}{ds} \left\{ (\tau + \tau' + \tilde{\tau}) \frac{d\tilde{v}}{ds} \right\} = m \frac{\partial^2 \tilde{v}}{\partial t^2} \tag{22}$$

$$\frac{d}{ds} \left\{ (\tau + \tau' + \tilde{\tau}) \left(\frac{dz}{ds} + \frac{dw}{ds} + \frac{d\tilde{w}}{ds} \right) \right\} = m \frac{\partial^2 \tilde{w}}{\partial t^2} - mg \tag{23}$$

where \tilde{u} , \tilde{v} , \tilde{w} are the longitudinal, out-of-plane and vertical dynamic components. $\tilde{\tau}$ is the additional dynamic tension inside the cable. We apply the same simplifications as before. The longitudinal component displacement is neglected as in the previous subsection. The equations are linearized by assuming that superimposed dynamic perturbations are small. After substituting the equations of static equilibrium, the equations of motion with harmonic time dependence are finally reduced to

$$(H + h) \frac{d^2 \tilde{v}}{dx^2} + m\omega^2 \tilde{v} = 0 \quad (24)$$

$$(H + h) \frac{d^2 \tilde{w}}{dx^2} + m\omega^2 \tilde{w} = \frac{mg}{H + h} \tilde{h} \quad (25)$$

\tilde{h} is the external dynamic tension. The boundary conditions for the dynamics are given by

$$\tilde{u}(0) = \tilde{h}/k_0, \quad \tilde{u}(l) = -\tilde{h}/k_l, \quad \tilde{v}(0) = \tilde{v}(l) = 0, \quad \tilde{w}(0) = \tilde{w}(l) = 0 \quad (26)$$

Following the same procedure as in the previous subsection, the application of Hooke's law yields after linearization the following equation for \tilde{h} :

$$\frac{\tilde{h}}{EA} \left(\frac{ds}{dx} \right)^3 = \frac{d\tilde{u}}{dx} + \left(\frac{dz}{dx} + \frac{dw}{dx} \right) \frac{d\tilde{w}}{dx} \quad (27)$$

and after integration

$$\frac{\tilde{h}L_e}{E_{eq}A_{eq}} = \frac{mg}{H + h} \int_0^l \tilde{w} dx \quad (28)$$

Out-of-plane motion: The eigensolutions of Eq. (24) together with the boundary conditions (26) are straightforward:

$$\Omega'_n = n\pi, \quad \tilde{v}_n(x) = C_n \sin \frac{n\pi}{l} x \quad (29)$$

where $\Omega = \omega l(H/m)^{-1/2}$ and $\Omega' = \Omega(1 + h^*)^{-1/2}$ respectively denote the initial and modified dimensionless angular frequencies. n is a positive integer.

In-plane motion: For the solutions of Eq. (25) with boundary conditions (26), it is convenient to distinguish symmetric modes from antisymmetric ones. From Eq. (28), antisymmetric modes do not induce additional dynamic tension ($\tilde{h} = 0$), so that their natural frequencies and modeshapes are

$$\Omega'_n = 2n\pi, \quad \tilde{w}_n(x) = A_n \sin \frac{2n\pi}{l} x \quad (30)$$

For the calculation of symmetric modes, one needs to find a peculiar solution of Eq. (25), which can simply be the constant $\tilde{h}g/\omega^2(H + h)$. After application of boundary conditions, it can be shown that the general solution for symmetric modes is

$$\tilde{w}_n(x) = \frac{mgl^2 \tilde{h}}{(H + h)^2 \Omega_n'^2} \left(1 - \tan \frac{\Omega'_n}{2} \sin \frac{\Omega'_n x}{l} - \cos \frac{\Omega'_n x}{l} \right) \quad (31)$$

Using Eq. (31) into (28), we obtained the following transcendental equation for the natural frequencies Ω'_n of symmetric modes:

$$\tan \frac{\Omega'}{2} = \frac{\Omega'}{2} - \frac{4}{\lambda'^2} \left(\frac{\Omega'}{2} \right)^3 \quad (32)$$

with $\lambda'^2 = \lambda^2/(1 + h^*)^3$. One remarks that this equation is the same as the well-known transcendental equation of Irvine, but with differently defined dimensionless parameters Ω' and λ'^2 (for $h^* = 0$, Irvine's equation is exactly recovered).

3. Results

The quantity of interest is the relative change in natural frequency due to temperature for a given cable (fixed λ^2). Frequency values without thermal stress are well-known [1]. For clarity, their evolution with respect to the sag-extensibility parameter is recalled in Fig. 2 (given Eq. (32), this figure also corresponds to the evolution of Ω' vs. λ'^2). Provided that one is interested in relatively low temperature change (typically due to climatic variations), the influence of temperature on material properties is neglected in the following results (without loss of generality for the proposed theory).

The only independent parameters of the problem are λ^2 and θ , so that quite general results are obtained through two-dimensional contour plots of $\Delta\omega/\omega = f(\lambda^2, \theta)$, where $\Delta\omega/\omega = \omega(\lambda^2, \theta)/\omega(\lambda^2, 0) - 1$ is the relative change in natural frequency under the influence of temperature. It is intuitively clear that for a fixed temperature change ΔT , the ratio H/EA must be low enough in order to have a non-negligible value of θ —and hence a non-negligible effect of

temperature on frequencies. In other words, cables that are strongly pre-tensioned will be less sensitive to temperature change. In this paper, Eqs. (20) and (32) are solved with a Newton–Raphson algorithm for λ^2 varying from 1 to 200 and θ varying from -1 to $+1$.

For out-of-plane and antisymmetric in-plane modes, the relative change in natural frequency is analytically obtained in terms of h^* as

$$\Delta\omega/\omega = \sqrt{1+h^*} - 1 \tag{33}$$

Fig. 3 gives the contour plots for $\sqrt{1+h^*} - 1$ ($\times 100$) in terms of θ and $\log \lambda^2$. For every value of λ^2 , the eigenfrequencies of such modes decrease as the temperature change increases. One can observe a slightly higher sensitivity to cooling than heating. However, for fixed values of θ , this sensitivity to temperature becomes lower and lower for cables having a larger and larger value of λ^2 . Note that comparing temperature sensitivity for different values of λ^2 at fixed θ implies that the ratio between the working stress H/A and Young’s modulus E should remain almost constant. For a given cable material, comparisons for fixed θ are hence indeed made for an almost constant safety factor, which is meaningful.

For symmetric in-plane modes, Eq. (32) must be solved. The effect of temperature on frequencies manifests itself through a modification of the axial tension (as for out-of-plane and antisymmetric modes) as well as through a sag modification, yielding a modified parameter λ'^2 as shown by Eq. (32). Fig. 4 plots the relative change of the first symmetric natural frequency. The thermal behaviour of this mode is strongly dependent on λ^2 and quite different from Fig. 3. Roughly, the frequency relative change is rather small above $\log \lambda^2 = 4.5$ ($\lambda^2 \simeq 90$). Between 2.5 and 4.5 (λ^2 between 12 and 90), it is more pronounced and the frequency is counterintuitively increasing with temperature. As shown later, such increase can lead to cross-over.

Below $\log \lambda^2 = 2.5$ ($\lambda^2 \simeq 12$), the behaviour changes again. For $\theta < 0$ (cooling), the first frequency is increasing as the temperature is decreasing. However, for $\theta > 0$ (heating), the modal behaviour is more complex: the frequency might increase or decrease depending on the value of λ^2 as well as of θ . Note that in certain region, the frequency is not

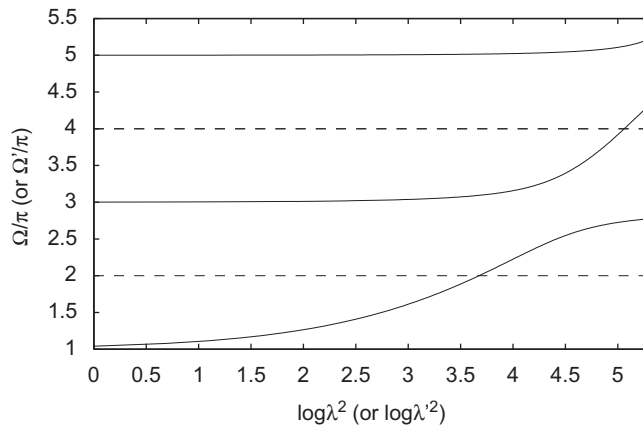


Fig. 2. Irvine’s natural frequencies vs. sag-extensibility parameter for the first three symmetric modes (solid lines) and the first two antisymmetric modes (dashed lines). Out-of-plane modes are not shown.

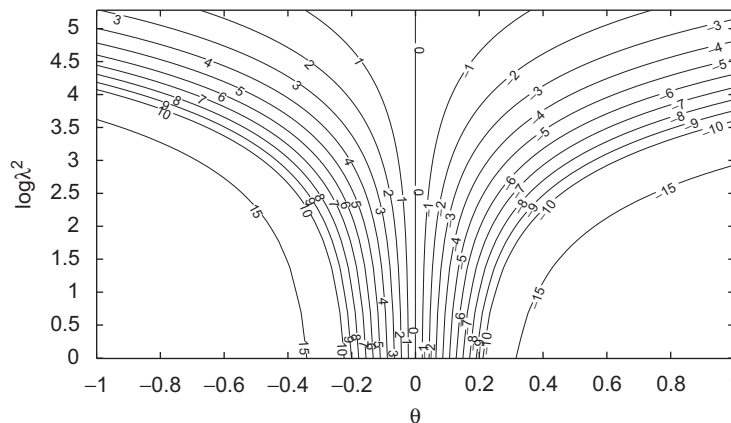


Fig. 3. Relative change in natural frequency ($\times 100$) for out-of-plane and in-plane antisymmetric modes.

monotonically varying with respect to temperature change, as it is the case for $\log \lambda^2 = 2$ ($\lambda^2 \simeq 7$) for instance: the frequency tends to increase for any negative or positive temperature change.

The fact that the frequency can increase with temperature is explained as follows. A temperature change modifies the axial tension as well as the cable sag. When the temperature increases, the axial tension always decreases while the sag-to-span always increases (as shown by Eqs. (12) and (33) together with the results of Fig. 3). A decrease of tension tends to decrease all natural frequencies, while the increase of sag tends to increase the frequencies of symmetric in-plane eigenmodes: tension and sag actions have hence a counteracting effect. This can be formally proven from Fig. 2: one has $\Omega'_n = f(\lambda^2)$, where f is a monotonically increasing function, which can be rewritten as

$$\Omega_n = f\left(\frac{\lambda^2}{(1+h^*)^3}\right)\sqrt{1+h^*} \quad (34)$$

Hence when h^* is decreasing (increasing temperature), the term $\sqrt{1+h^*}$ decreases while the function $f(\cdot)$ increases: this means that the decrease of tension can be compensated by the increase of the sag-extensibility parameter. Note that for taut strings ($\lambda^2 = 0$), frequencies are given by $\Omega_n = n\pi\sqrt{1+h^*}$ and hence always decrease for positive thermal changes (their relative change is the same as in Fig. 3).

Figs. 5 and 6 also give the contour plots for the relative change in frequency of the second and third in-plane symmetric modes. As for the first mode, their thermal behaviour is still significantly different from antisymmetric modes. However, differences become weaker as the mode order increases and the behaviour tends to become identical to that of antisymmetric and out-of-plane modes (compare Fig. 6 with Fig. 3).

As a last example, one considers a cable subjected to a temperature change ranging from -40 to $+40$ K. The cable has the following characteristics: $l = 200$ m, $A = 7.069e - 2$ m², $E = 2.0e + 11$ Pa, $\rho = 7800$ kg m⁻³, $\alpha = 1.2e - 5$ K⁻¹, $g = 9.81$ m s⁻². The initial applied tension is $H = 0.938e + 7$ N so that $\lambda^2 = 20.01$ and θ ranges from -0.723 to $+0.723$.

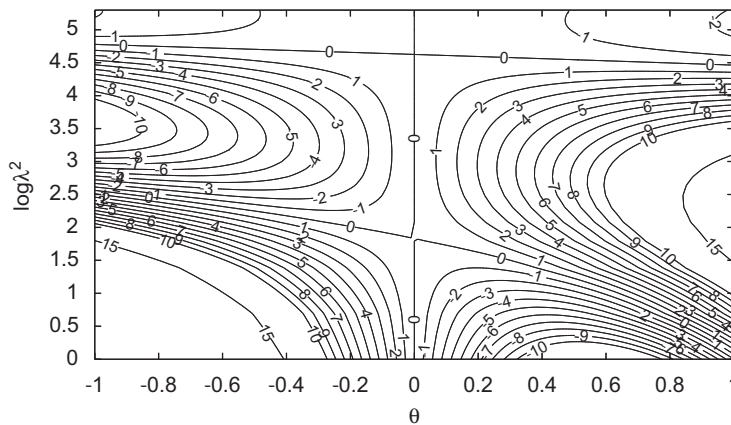


Fig. 4. Relative change in natural frequency ($\times 100$) for the first in-plane symmetric mode.

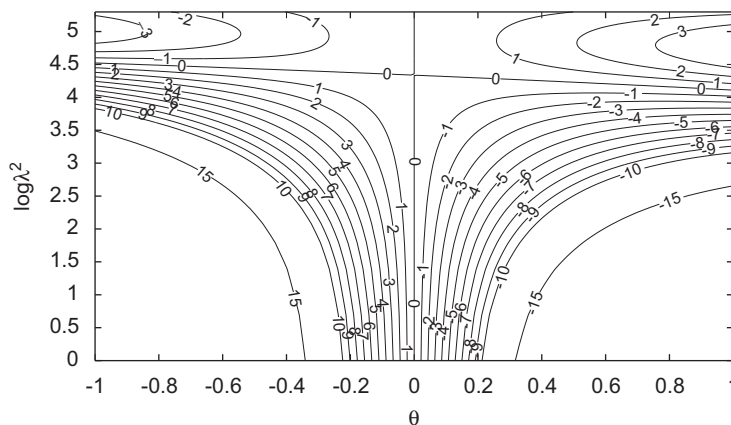


Fig. 5. Relative change in natural frequency ($\times 100$) for the second in-plane symmetric mode.

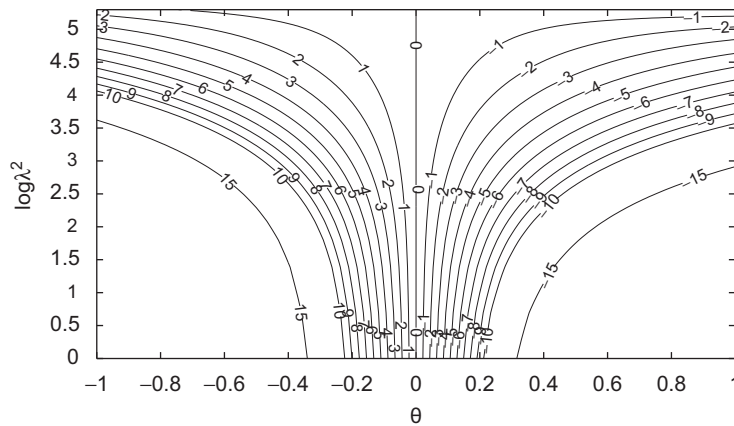


Fig. 6. Relative change in natural frequency ($\times 100$) for the third in-plane symmetric mode.

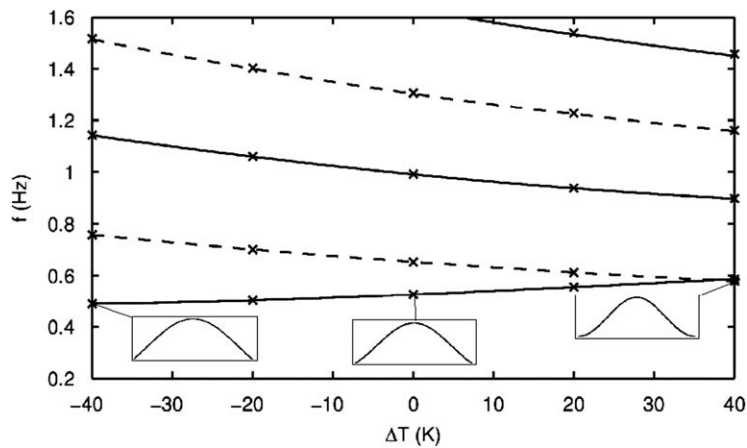


Fig. 7. Natural frequencies vs. temperature change for the first three symmetric modes (solid lines) and the first two antisymmetric modes (dashed lines). Out-of-plane modes not shown for clarity. Insets: first symmetric modeshapes for -40 , 0 and $+40$ K. \times -mark: finite element solution.

Horizontal supports are supposed to have infinite stiffness. Fig. 7 exhibits the evolution of the first in-plane eigenfrequencies vs. temperature change. Excepted the first one, all natural frequencies are decreased with heating. The frequency relative change for the first and second symmetric modes respectively varies from -7.0 to $+11.6$ percent and $+15.2$ to -9.5 percent, while it varies from $+16.1$ to -11.3 percent for antisymmetric modes (these values can be also directly found from Figs. 3–5). Also sketched in Fig. 7, the evolution of the first modeshape appears to be significant. Indeed, one cross-over between the first symmetric and antisymmetric modes occurs near $+40$ K. This due to the fact that for ΔT varying from -40 to $+40$ K, the modified Irvine parameter λ^2 ranges from 8.17 to 40.97 , which is greater than the well-known cross-over value of $4\pi^2$. In the present example, it should be noticed that cable end supports were supposed to have infinite stiffness and to remain fixed with respect to temperature, which maximizes thermal effects. In real situations, the behaviour of end supports is more complicated and usually depends on the thermomechanical behaviour of the cable structure as a whole.

In order to check the validity of the above results, a comparison with finite element solutions is finally performed (see Fig. 7 also). Finite element solutions have been obtained from a planar Euler–Bernoulli beam model developed by the author in Ref. [21] for studying the effect upon vibrations of thermal stress including initial bend. The beam has been discretized into 100 elements. Simple supports have been used as well as a negligible bending stiffness ($I = 5.8908e - 5 \text{ m}^4$, yielding a high bending stiffness parameter [3,4] $\xi = \sqrt{HI^2/EI} = 178$). As can be observed in Fig. 7, results obtained with the proposed cable model are in quite good agreement with numerical results.

4. Conclusion

In this paper, the analytical model of Irvine has been extended to thermoelasticity. The effect of thermal stress typically due to climatic change on cable free vibrations has been investigated. Some general two-dimensional contour plots have

been presented for the relative change in natural frequencies due to temperature with respect to the only two independent parameters of the problem. Depending on the values of λ^2 and θ , thermal stress is likely to have a quite significant effect on natural frequencies as well as modeshapes. For in-plane symmetric modes, it has been shown that a positive (resp. negative) temperature change does not necessarily decrease (resp. increase) natural frequencies and that thermoelastic effects can produce sag modifications that can lead to cross-over. As a consequence, the thermoelastic behaviour of cables is likely to affect the robustness of vibration based methods in SHM. Future studies should deal with the influence of bending stiffness, which cannot generally be neglected for higher-order modes or large-diameter cables.

References

- [1] H.M. Irvine, *Cable Structures*, The MIT Press, Cambridge, NJ, 1981.
- [2] M.S. Triantafyllou, Linear dynamics of cables and chains, *The Shock and Vibration Digest* 16 (1984) 9–17.
- [3] A.B. Mehrabi, H. Tabatabai, Unified finite difference formulation for free vibration of cables, *Journal of Structural Engineering* 124 (1998) 1313–1322.
- [4] Y.Q. Ni, J.M. Ko, G. Zheng, Dynamic analysis of large-diameter sagged cables taking into account flexural rigidity, *Journal of Sound and Vibration* 257 (2002) 301–319.
- [5] G. Rega, Nonlinear vibrations of suspended cables. Part i: modeling and analysis; part ii: deterministic phenomena, *Applied Mechanics Reviews* 57 (2004) 443–514.
- [6] N. Srinil, G. Rega, S. Chuecheepsakul, Three-dimensional non-linear coupling and dynamic tension in large-diameter free vibrations of arbitrary sagged cables, *Journal of Sound and Vibration* 269 (2004) 823–852.
- [7] Z.H. Zhu, S.A. Meguid, Elastodynamic analysis of low tension cables using a new curved beam element, *International Journal of Solids and Structures* 43 (2006) 1490–1504.
- [8] N. Srinil, G. Rega, Nonlinear longitudinal/transversal modal interactions in highly extensible suspended cables, *Journal of Sound and Vibration* 310 (2008) 230–242.
- [9] G. Rega, N. Srinil, R. Alaggio, Experimental and numerical studies of inclined cables: free and parametrically-forced vibrations, *Journal of Theoretical and Applied Mechanics* 46 (2008) 621–640.
- [10] W.X. Ren, G. Chen, W.H. Hu, Empirical formulas to estimate cable tension by cable fundamental frequency, *Structural Engineering and Mechanics* 20 (2005) 363–380.
- [11] B.H. Kim, T. Park, Estimation of cable tension force using the frequency-based system identification method, *Journal of Sound and Vibration* 304 (2007) 660–676.
- [12] N. Bouaanani, Numerical investigation of the modal sensitivity of suspended cables with localized damage, *Journal of Sound and Vibration* 292 (2006) 1015–1030.
- [13] M. Lepidi, V. Gattulli, F. Vestroni, Static and dynamic response of elastic suspended cables with damage, *International Journal of Solids and Structures* 44 (2007) 8194–8212.
- [14] R.G. Rohrmann, M. Baessler, S. Said, W. Schmid, W. Ruecker, Structural causes of temperature affected modal data of civil structures obtained by long time monitoring, *Proceedings of the 18th International Modal Analysis Conference (IMAC)*, San Antonio, USA, 2000, pp. 1–7.
- [15] B. Peeters, J. Maeck, G.D. Roeck, Vibration-based damage detection in civil engineering: excitation sources and temperature effects, *Smart Materials and Structures* 10 (2001) 518–527.
- [16] E. Balmès, M. Basseville, F. Bourquin, L. Mevel, H. Nasser, F. Treyssède, Merging sensor data from multiple temperature scenarios for vibration monitoring of civil structures, *Structural Health Monitoring* 7 (2008) 129–142.
- [17] A. Deraemaeker, E. Reynders, G.D. Roeck, J. Kullaa, Vibration-based structural health monitoring using output-only measurements under changing environment, *Mechanical Systems and Signal Processing* 22 (2008) 34–56.
- [18] S. Na, L. Librescu, H. Jung, Dynamics and active bending vibration control of turbomachinery rotating blades featuring temperature-dependent material properties, *Journal of Thermal Stresses* 27 (2004) 625–644.
- [19] M. Parris, F. Curti, D.D. Rosa, Dynamic response of a system driven by thermal actuation, *Advances in the Astronautical Sciences, Space Flight Mechanics 2004*, Vol. 119, 2005, pp. 821–832.
- [20] B.A. Boley, J.H. Wiener, *Theory of Thermal Stresses*, Wiley, New York, 1960.
- [21] F. Treyssède, Prebending effects upon the vibrational modes of the thermally prestressed planar beams, *Journal of Sound and Vibration* 307 (2007) 295–311.